Published in final edited form as:
Dev Biol. 2014 November 1; 395(1): 50–61. doi:10.1016/j.ydbio.2014.08.030.

FOG-2 Mediated Recruitment of the NuRD Complex Regulates Cardiomyocyte Proliferation during Heart Development

Audrey S. Garnatz[3], **Zhiguang Gao**[1], **Michael Broman**[2], **Spencer Martens**[2], **Judy U. Earley**[2], and **Eric C. Svensson**[2,3]

[1]Department of Biochemistry and Molecular Biology, The University of Texas MD Anderson Cancer Center, Houston, TX 77030

[2]Department of Medicine, The University of Chicago, Chicago, IL 60637

[3]Committee on Development, Regeneration, and Stem Cell Biology, The University of Chicago, Chicago, IL 60637

SUMMARY

FOG-2 is a multi-zinc finger protein that binds the transcriptional activator GATA4 and modulates GATA4-mediated regulation of target genes during heart development. Our previous work has demonstrated that the Nucleosome Remodeling and Deacetylase (NuRD) complex physically interacts with FOG-2 and is necessary for FOG-2 mediated repression of GATA4 activity *in vitro*. However, the relevance of this interaction for FOG-2 function *in vivo* has remained unclear. In this report, we demonstrate the importance of FOG-2/NuRD interaction through the generation and characterization of mice homozygous for a mutation in FOG-2 that disrupts NuRD binding (FOG-2^{R3K5A}). These mice exhibit a perinatal lethality and have multiple cardiac malformations, including ventricular and atrial septal defects and a thin ventricular myocardium. To investigate the etiology of the thin myocardium, we measured the rate of cardiomyocyte proliferation in wild-type and FOG-2^{R3K5A} developing hearts. We found cardiomyocyte proliferation was reduced by 31 ± 8% in FOG-2^{R3K5A} mice. Gene expression analysis indicated that the cell cycle inhibitor *Cdkn1a* ($p21^{cip1}$) is up-regulated 2.0 ± 0.2-fold in FOG-2^{R3K5A} hearts. In addition, we demonstrate that FOG-2 can directly repress the activity of the *Cdkn1a* gene promoter, suggesting a model by which FOG-2/NuRD promotes ventricular wall thickening by repression of this cell cycle inhibitor. Consistent with this notion, the genetic ablation of *Cdkn1a* in FOG-2^{R3K5A} mice leads to an improvement in left ventricular function and a partial rescue of left ventricular wall thickness. Taken together, our results define a novel mechanism in which FOG-2/NuRD interaction is required for cardiomyocyte proliferation by directly down-regulating the cell cycle inhibitor *Cdkn1a* during heart development.

Address correspondence to: Eric C. Svensson, M.D., Ph.D. Translational Medicine Novartis Institutes for Biomedical Research 220 Massachusetts Avenue Cambridge, MA, USA Phone: (617) 871-3108 Fax: (617) 871-7486 eric.svensson@novartis.com.

Keywords

Chromatin; Zfpm2; Cdkn1a

INTRODUCTION

FOG-2 is a transcriptional co-factor that is known to play important roles in cardiac, gonadal, and pulmonary development. It is expressed in the heart during mid and late gestation, and then continues to be expressed at a low level in the adult heart (Lu et al., 1999; Svensson et al., 2000a; Svensson et al., 1999; Tevosian et al., 1999). Most of its functions in heart development are mediated through interaction with the transcriptional activator GATA4 (Crispino et al., 2001). FOG-2 deficient mice die between embryonic day (E) 13.5 and 14.5 from heart failure due to cardiac malformations. These cardiac structural abnormalities include a large common AV valve, atrial and ventricular septal defects, hyperplastic endocardial cushions, an overriding aorta, and a thin compact zone of the ventricular myocardium (Svensson et al., 2000b; Tevosian et al., 2000). In addition, mice deficient in FOG-2 fail to form a subepicaridal capillary plexus, the precursor to the mature coronary vasculature (Tevosian et al., 2000).

In most cell and promoter contexts, the interaction of FOG-2 with GATA4 results in the transcriptional repression of target genes. This occurs in part through the FOG-2 mediated recruitment of other transcriptional repressive complexes and factors to target promoters. One such transcriptional repressor is C-terminal binding protein (CtBP), which physically interacts with FOG-2 via a motif in the C-terminal half of the FOG-2 protein. However, this interaction does not seem to be required for repression of target genes *in vitro*, and it is unclear what role this interaction may play *in vivo* (Holmes et al., 1999; Katz et al., 2002; Svensson et al., 2000a). FOG-2 has also been shown to interact with COUP-TFII *in vitro*, though the significance of this interaction *in vivo* is also unknown (Huggins et al., 2001).

We have previously shown that the N-terminus of FOG-2 is required for repression of FOG-2 targets *in vitro*, and that the 12 N-terminal amino acids of FOG-2 are sufficient to mediate repression of a promoter when fused to a DNA binding domain (Lin et al., 2004; Svensson et al., 2000a). This 12 amino acid motif is not required for FOG-2's interaction with GATA4 or CtBP, and instead has been shown to interact with components of the Nucleosome Remodeling and Deacetylase (NuRD) complex. This motif is found not only in both FOG-1 and FOG-2, but also at the N-termini of other transcriptional modulators, some of which have roles in the regulation of heart development, such as SALL1 and SALL4 (Bruneau, 2008; Gao et al., 2010a; Hong et al., 2005; Kiefer et al., 2008; Lin et al., 2004; Roche et al., 2008; Sakaki-Yumoto et al., 2006).

The NuRD complex has eight subunits: Mi2ß, RbAp46, RbAp48, p66, MTA1, 2, or 3, and MBD3 (Wade et al., 1998; Xue et al., 1998; Zhang et al., 1998). The N-terminus of both FOG-1 and FOG-2 has been shown to physically interact with the MTA and RbAp subunits of the NuRD complex both *in vitro* and *in vivo*. Mutation of critical residues within this motif abolished binding to NuRD subunits, and knock-down of MTA subunits *in vitro* abolished FOG-2-mediated repression (Hong et al., 2005; Roche et al., 2008). The structure

of the interaction between the FOG repression motif of FOG-1 and RbAp48 has been recently determined using xray crystallography, confirming the key amino acids in FOG proteins required for FOG-NuRD interaction (Lejon et al., 2011). Previously, we have described the generation and characterization of a mouse engineered to carry specific mutations in the gene encoding FOG-1 (FOG-1^{R3K5A}) that disrupts the ability of FOG-1 to interact with the NuRD complex. Mice homozygous for these mutations developed defects in hematopoetic development, demonstrating the importance of FOG-1/NuRD interactions for the maturation of megakaryocytes and erythrocytes *in vivo* (Gao et al., 2010a; Miccio et al., 2010).

To explore the importance of FOG-2/NuRD interactions for the regulation of cardiac development, we set out to generate mice with a targeted mutation in the gene encoding FOG-2 (*Zfpm2*, hereafter referred to as FOG-2) that would disrupt the FOG-2/NuRD interaction *in vivo*. In this report, we demonstrate that mice homozygous for such a mutation (FOG-2^{R3K5A}) have a near complete perinatal lethality. The hearts of these mice have a membraneous ventricular septal defect and left ventricular dysfunction due to a hypoplastic ventricular myocardium. Further, we demonstrate upregulation of the cell-cycle inhibitor *Cdkn1a* (p21^{cip1}) in FOG-2^{R3K5A} hearts due to a failure of mutant FOG-2 to repress the *Cdkn1a* promoter resulting from loss of FOG-2/NuRD interaction. Genetically ablating *Cdkn1a* is able to partially rescue the FOG-2^{R3K5A} phenotype, demonstrating that FOG-2 modulation of *Cdkn1a* expression is critical for the regulation of cardiomyocyte proliferation during cardiac development.

MATERIALS AND METHODS

Generation of FOG-2$^{R3K5A/R3K5A}$mice

Recombineering techniques were used to create a vector harboring the R3K5A mutation in the first exon of the gene encoding FOG-2 while also adding a novel SacI restriction site (Liu et al., 2003). The vector was linearized and electroporated into 129 S6/SvEv ES cells, clones of which were then screened using Southern analysis for homologous recombination at the *Zfpm2* locus using genomic probes outside the targeting vector from both the 5’ and 3’ ends of the allele. ES cells that were correctly targeted were then injected into C57BL/6 blastocysts to generate chimeric mice. These mice were then bred further to obtain germline transmission of the targeted allele. Heterozygotes were then bred with Prmcre transgenic mice from the Jackson laboratory (129S/Sv-Tg(Prm-cre)580g/J) to excise the neomycin cassette from the allele, generating the FOG-2^{R3K5A} allele (see Figure 1). For rescue experiments, FOG-2$^{R3K5A/+}$ heterozygotes were crossed to *Cdkn1a*$^{-/-}$ mice (line B6;129S2-Cdkn1atn1Tyj/J:JAX) obtained from the Jackson Laboratory, after which double heterozygotes were interbred. All mouse work was performed at the University of Chicago according to the animal care and use guidelines.

Western Analysis

Twenty-five micrograms of whole heart lysate from E13.5 mouse embryos from either wild-type, mutant, or heterozygote siblings was resolved on a 7% SDS-PAGE gel and transferred to a nitrocellulose membrane (Whatman, Piscataway NJ). The membrane was then blocked

as previously described (Gao et al., 2010b) and incubated with 1:1000 dilution of rabbit anti-FOG-2 antibody (M247, Santa Cruz Biotechnology) rocking overnight at 4°C, then washed and incubated with HRP-coupled goat anti-rabbit IgG diluted 1:5000 (Jackson ImmnoResearch) for 3 hours at room temperature. The membrane was developed using the ECL-plus kit (Amersham) and exposed to film. To assure equal protein loading between lanes, the membrane was then stripped and re-probed for HSP90 using a 1:5000 dilution of a rabbit anti-HSP90 antibody (H-114, Santa Cruz Biotechnology).

Transient transfection and promoter analysis

p638ANF-Luc, pcDNA-FOG-2, pcDNAGATA4, pVR-beta-galactosidase have been described previously (Knowlton et al., 1991; Svensson et al., 1999), pcDNA-FOG-2^{R3K5A} was created by making a targeted mutation in pcDNA-FOG-2 using PCR with primers (5'-GAAATGTCCGCGCGAGCTCAGAGTAAACCC CGGCAGATCAAACG and 5'-TACTCTGAGCTCGCGCGGACATTTCGGCCGCGGCCGCT GCCGCTG), resulting in a mutant version of FOG-2 that encodes alanine at amino acid position 3 and 5 instead of arginine and lysine, respectively. After construction, the vector was sequenced to confirm creation of pcDNA-FOG2^{R3K5A}. The construct p21-Luc was generated by tailed PCR of 2kb of the *Cdkn1a* promoter region using the following tailed primers: 5'-CGGCTCGAGTGTCTAGGTCAGCTAAATCCGAGG and 5'-CGCAAGCTTAAGCTCTCAC CTCTGAATGTCTGG. The resultant PCR product was then digested with XhoI and HindII, ligated into pGL2basic vector, and confirmed by sequencing to create p21-Luc reporter plasmid. Transient transfection into NIH 3T3 fibroblasts was performed as previously described (Kim et al., 2009). Cells were harvested and lysed with 100uL/well of Reporter Lysis Buffer (Promega). Cell lysates were then frozen at −20°C and thawed before assay in the Glomax 20/20 Luminometer (Promega) using 20uL of cell lysate and 100uL Luciferase Assay Substrate (Promega). Beta-galactosidase activity assays were performed as described previously (Kim et al., 2009; Lin et al., 2004). Luciferase activity was normalized to β-galactosidease activity to control for transfection efficiency. Each experiment was performed in triplicate in three independent experiments and results presented as the mean ± S. E. M. A Student's t-test was performed between each set of experimental conditions to determine statistical significance.

Echocardiography

Newborn FOG-2^{R3K5A} pups were subject to echocardiography using a VisualSonics Vevo 770 machine with a 30 MHz transducer. Mice were placed on a 37°C warming pad and lightly sedated with 1% isoflurane. Conscious imaging was performed to acquire two-dimensional parasternal short axis M-mode images. Percent left ventricular fractional shortening was calculated as [(diastolic left ventricular internal diameter- systolic left ventricular internal diameter)/diastolic left ventricular internal diameter]*100. A Student's t-test was performed between each set of experimental conditions to determine statistical significance.

Microarray Data and Analysis

Affymetrix GeneChip Mouse Genome 430 2.0 microarrays were used for analysis of expression of RNA isolated from E16.5 wild-type and FOG-2^{R3K5A} whole hearts. This microarray data is available under accession GSE50426 in the GEO database. Analysis of results was performed using dChip (Li and Wong, 2001) and Ingenuity Pathway Analysis (IPA) software (Ingenuity Systems). dChip identified 670 probe sets that were misregulated by at least 1.3-fold in the FOG-2^{R3K5A} hearts. Using these probe sets, IPA identified 41 networks consisting of 332 misregulated focus molecules. Three hundred ten of the original 332 focus molecules fell into 19 networks containing more than one focus molecule. We grouped the networks with multiple focus molecules into 7 super-networks based on the descriptions of network function provided by IPA (Supplementary Table 2).

In order to generate a heat map of mis-regulated cell cycle genes, we generated a list of genes on the microarray chip associated with the following gene ontology terms: regulation of cell cycle, positive regulation of cell cycle, negative regulation of cell cycle, mitosis, cell proliferation, cell division, and cell cycle. We then used dChip to identify the genes on this list that were misregulated at least 1.3-fold. Hierarchical clustering by dChip was used to generate a heatmap of these genes to visualize the trends in their misregulation.

Proliferation Assays

To measure the rate of cardiomyocyte proliferation in the hearts of developing embryos, we developed an immunofluorescence approach to co-stain histologic sections from E16.5 mouse embryos with antibodies to phosphohistone-H3 (PH3, Cell Signaling) to mark proliferating cells, and to myosin heavy chain (MF20, Developmental Studies Hybridoma Bank, University of Iowa) to mark cardiomyocytes. Briefly, sections were prepared, processed, and incubated with an anti-phosphohistone H3 antibody as described previously (Flagg et al., 2007). Following this incubation, sections were washed and incubated overnight at 4°C with the MF20 antibody diluted 1:100 in a blocking solution of 1% BSA and 5% normal goat serum in PBS. The sections were then washed 3 times for 15 minutes in PBS, and a Donkey anti-Mouse antibody conjugated to Cy3 (715-165-150, Jackson ImmunoResearch) was added to the slides at a 1:200 dilution concurrently with the secondary antibody for PH3 (Flagg et al., 2007). Following this incubation, sections were washed with PBS, co-stained with DAPI, and then immunofluorescence was visualized using a Zeiss Axiphot fluorescence microscope. Digital images were captured and cell counting of DAPI-stained cell nuclei was performed in Image J. Phosphohistone-H3 positive cells that were also MF-20 positive were counted manually. The proliferation index was calculated by dividing the number of mitotic cardiomyocytes (cells stained by both MF20 and PH3) by the total number of DAPI-positive cells in the ventricular myocardium of each section. At least 7 sections from each heart were analyzed from each of 3 wild type and 3 mutant embryos. A Student's t-test was performed between each set of experimental conditions to determine statistical significance.

Quantitative RT-PCR

Hearts from E16.5 embryos were harvested in RNAse-free conditions and frozen in liquid nitrogen, then divided into three biological replicates of each genotype, containing at least

two hearts in each replicate. Total RNA was then extracted with Trizol (Invitrogen) and cDNA was prepared with qScript cDNA SuperMix (Quanta Biosciences, Gaithersburg MD). Quantitative PCR was then performed using DyNAmo HS SYBR Green qPCR kit (Thermo Fisher Scientific, Waltham MA), with primers as listed in Supplementary Table 1 for at least three independent experiments on each biological replicate. Results were analyzed using the previously described methods (Gao et al., 2010b; Tichopad et al., 2003) and were normalized to levels of *Gapdh* to control for variation in cDNA quantity. A Student's t-test was performed between each set of experimental conditions to determine statistical significance.

Quantitation of Ventricular Wall Thickness

Wild-type, FOG-2^{R3K5A}, and FOG-2^{R3K5A};*Cdkn1a*$^{-/-}$ double mutant newborn mice were harvested, fixed in 10% formalin, and embedded in paraffin. Transverse sections through the hearts were then prepared and stained with hemotoxylin and eosin. Photographs of comparable sections were obtained using a Zeiss Axiophot microscope. Left ventricular wall thickness was measured from the base of the trabecular zone to the epicardium from 8 sections each from 3 hearts of each genotype at the thinnest point of the apical-lateral wall of the left ventricle. Results are reported as the mean ± S.E.M. for each genotype. A Student's t-test was used to determine statistical significance.

RESULTS

A mutation in the N-terminal motif of FOG-2 abrogates FOG-2 mediated repression of GATA- 4 induced transcriptional activity

As we and others have previously shown, the first 12 N-terminal amino acids of FOG-1 and FOG-2 are highly conserved and are required for full repressive activity of both FOG-1 and FOG-2 (Hong et al., 2005; Lin et al., 2004; Roche et al., 2008; Svensson et al., 2000a). These amino acids, termed the FOG repression motif, physically interact with the MTA and RbAp components of the NuRD complex, resulting in the recruitment of the NuRD complex to target promoters (Gao et al., 2010a; Roche et al., 2008). Mutation of amino acids within this motif results in a loss of binding to MTA and RbAp proteins and a loss of repressive activity *in vitro* (Gao et al., 2010a; Hong et al., 2005; Roche et al., 2008). Further, generation of mice with substitution of the 3rd and 5th amino acids for alanine (R3K5A) in FOG-1 results in the failure to recruit the NuRD complex to target promoters and the attenuation of FOG-1 target gene repression *in vivo* (Gao et al., 2010a; Miccio et al., 2010).

To confirm that a similar mutation in the gene encoding FOG-2 also blocks FOG-2-mediated transcriptional repression, we generated a mammalian expression vector that encodes FOG-2 with the R3K5A mutation (pcDNA-FOG-2^{R3K5A}). We then transiently transfected NIH3T3 cells, which endogenously express the components of the NuRD complex, with a vector containing the atrial naturetic factor (ANF) promoter driving expression of the reporter gene luciferase. In addition, we also included expression vectors for the transcriptional activator GATA4 as well as FOG-2 (Supplemental Figure 1). In the presence of GATA4, the ANF promoter was activated 139 ± 36 fold. Further, the addition of wild-type FOG-2 resulted in an almost complete repression of GATA4-mediated

transactivation of the ANF promoter. In contrast, expression of the FOG-2^{R3K5A} protein was unable to significantly repress GATA-4 activated transcription of the ANF promoter in NIH3T3 cells in this transient transfection assay. These results are consistent with our previous results and show the importance of these residues for FOG-2 mediated repression by the NuRD complex (Gao et al., 2010a; Lin et al., 2004; Roche et al., 2008; Svensson et al., 2000a).

Creating a mouse harboring the FOG-2^{R3K5A} mutation

In order to determine the importance of FOG-2/NuRD interactions in heart development, we created a mouse harboring the R3K5A mutation in the endogenous *Zfpm2* locus that would produce a mutant version of FOG-2 unable to interact with the NuRD complex *in vivo* (Figure 1A). Exon 1 of the *Zfpm2* gene encodes the translational start site and the first 13 amino acids of FOG-2. Using site directed mutagenesis on a plasmid containing this region of the FOG-2 gene, mutations in 5 base pairs were introduced resulting in the generation of a novel SacI site in Exon 1. This also resulted in a change in the codons corresponding to amino acids 3 and 5 of FOG-2, changing them from arginine and lysine to alanine. This plasmid was then used to generate an ES cell targeting vector which was transfected into murine ES cells. Neomycin-resistant ES cell clones were screened using Southern analysis for ES cells that had undergone homologous recombination at the *Zfpm2* locus (data not shown). Correctly targeted ES cells were microinjected into blastocysts to generate chimeric mice. These chimeras were then bred to achieve germline transmission of the target locus as demonstrated by Southern analysis (Figure 1B). The neomycin resistance cassette was removed from the altered *Zfpm2* locus by crossing mice carrying this allele to mice that express Cre in cells of their germline (Prm-cre transgenic mice). Cre-mediated excision of the targeted locus resulted in the removal of the neomycin cassette in the germline of the progeny from this cross, leaving behind the targeted mutations in exon 1 and just one loxP site in the first intron of the gene (Figure 1A, C).

FOG-2^{R3K5A} mice die perinatally

Mice heterozygous for the targeted allele lacking the neomycin cassette (FOG-2$^{R3K5A/+}$) are viable and fertile, exhibit no grossly apparent malformations, and have a normal lifespan. As a first step in our analysis of homozygous FOG-2$^{R3K5A/R3K5A}$ mice, we crossed male and female FOG-2$^{R3K5A/+}$ mice to generate FOG-2$^{R3K5A/R3K5A}$ mice (hereafter referred to as FOG-2^{R3K5A} mice) and analyzed the genotypes of the progeny from this cross at different times in development (Table 1). Our results demonstrate that FOG-2^{R3K5A} mice die shortly after they are born. *In utero*, the genotypes of embryos from crosses between heterozygotes conformed to a 1:2:1 Mendelian ratio. However, after birth, FOG-2^{R3K5A} mice were under-represented, and by weaning nearly all mutants were dead (Table 1). Those few FOG-2^{R3K5A} mice that survived to weaning died shortly thereafter, demonstrating a fully penetrant lethality of the FOG-2^{R3K5A} allele. Western analysis of E13.5 hearts demonstrated that the overall level of FOG-2 produced in wild-type hearts compared to FOG-2^{R3K5A} hearts is comparable (Figure 1D), suggesting that the critical regulatory elements controlling expression of FOG-2 were not perturbed by introduction of the targeted mutations.

Dilated Cardiomyopathy and Septal Defects in FOG2^{R3K5A} hearts

To determine the cause of the perinatal lethality in the FOG-2^{R3K5A} mice, we performed echocardiography on newborn pups (Figure 2). In mutant mice, we observed a trend toward an increase in left ventricular enddiastolic dimension (1.38 ± 0.06 mm vs. 1.62 ± 0.09 mm), a significant increase in left ventricular end-systolic dimension (0.73 ± 0.03 mm vs. 1.10 ± 0.06 mm, $p<0.001$), and a significant reduction in the fractional shortening (47.3 ± 1.5% vs 31.4 ± 1.6%, $p<0.0001$). Taken together, these results suggest that the FOG-2^{R3K5A} mice die of systolic heart failure. To look more closely at the hearts of FOG-2^{R3K5A} mice, we performed a histologic analysis (Figure 3). FOG-2^{R3K5A} hearts showed several morphogenic abnormalities. First, all FOG-2^{R3K5A} hearts had an ostium secundum atrial septal defect (ASD) (Figure 3A, B) and a membranous ventricular septal defect (VSD) (Figure 3C, D). Additionally, FOG-2^{R3K5A} hearts had a very thin, dilated left ventricular wall. Interestingly, the valves of FOG-2^{R3K5A} hearts appear to be grossly normal, unlike FOG-2 deficient mice, which have hyperplastic endocardial cushions by E12.5 (Flagg et al., 2007; Svensson et al., 2000b). Further, formation of coronary vascular plexus, which fails to develop in FOG-2 deficient mice (Tevosian et al., 2000), forms with only a slight delay in FOG-2^{R3K5A} hearts; at E13.5 the vessels are clearly not branching completely over the dorsal surface of the ventricles, but by E14.5 they appear normal (Supplemental Figure 2). This supports the notion that the R3K5A mutation only abrogates a subset of the functions performed by FOG-2 in development of the heart. Specifically, the N-terminal repression motif in FOG-2 is required to direct proper development of the ventricular and atrial septa and of the ventricular wall, but not of the coronary vasculature or the cardiac valves.

FOG-2^{R3K5A} mice have a cardiomyocyte proliferation defect during embryogenesis

In order to determine genes misregulated in FOG-2^{R3K5A} hearts that would explain the thin ventricular wall phenotype, we performed microarray analysis on wild-type and FOG-2^{R3K5A} hearts at E16.5, as this is developmental timepoint at which the FOG-2^{R3K5A} thin wall phenotype is first apparent on histological analysis (data not shown). This microarray data is available under accession GSE50426 in the GEO database. Analysis of the resultant data using dChip and Ingenuity Pathway Analysis software identified 19 gene networks containing more than one focus molecule misregulated by greater than 1.3-fold in the hearts of FOG-2^{R3K5A} mice. We then further grouped these 19 networks into 7 super-networks based on their functional description (Figure 4A, Supplemental Table 2). The super-networks with the most focus molecules have functions in cell proliferation and cell death, while the super-network with the third most focus molecules is associated with other general developmental processes (Figure 4A). Given these results and previous observations demonstrating the importance of cardiomyocyte proliferation during this time point in development (Ahuja et al., 2007), we hypothesized that the thin walled phenotype in the FOG-2^{R3K5A} mice was due to either a failure of cardiomyocyte proliferation or an abnormal increase in cardiomyocyte apoptosis.

In order to differentiate between these possibilities, we measured the rate of apoptosis and the rate of proliferation of cardiomyocytes in wild-type and FOG-2^{R3K5A} hearts at E16.5, the developmental timepoint when the walls first appear thinner by histology (data not shown). To measure apoptosis, we used an immunofluorescence-based assay to detect

TUNEL positive cells that also expressed myosin heavy chain on sections of E16.5 hearts from wild-type and FOG-2^{R3K5A} embryos (Supplemental Figure 3). Cardiomyocyte apoptosis was extremely rare in the developing heart and was not significantly altered in FOG-2^{R3K5A} hearts, demonstrating that an increase in apoptosis is not the cause of the thin ventricular compact zone. To examine cardiomyocyte proliferation in these mice, a similar approach was taken using an antibody against phosphohistone H3, a marker of proliferating cells (Figure 5). In wild-type embryos, cardiomyoctye proliferation was readily apparent, with an overall cardiomyocyte proliferation index of 0.663 ± 0.049 proliferating cells per 100. In contrast, the number of proliferating cardiomyocytes in FOG-2^{R3K5A} embryos was only 0.460 ± 0.024 cells per 100, a 31% decrease in FOG-2^{R3K5A} ventricles as compared to their wild-type littermates (Figure 5). This result strongly suggests that the thin ventricular wall seen in FOG-2^{R3K5A} hearts is due to a cardiomyocyte proliferation defect.

The cell-cycle inhibitor p21^{cip1} is significantly upregulated in mutant hearts and is a target of FOG-2/NuRD-mediated repression

To begin to elucidate the FOG-2 dependent molecular pathway that regulates cardiomyocyte proliferation, we re-examined our microarray data for clues that would explain a lack of cardiomyocyte proliferation. Using dChip and gene ontology analysis, we generated a heatmap of misregulated cell cycle and proliferation genes (Figure 4B). Since the NuRD complex is known to promote a closed chromatin state and repress gene expression, direct transcriptional targets of FOG-2/NuRD should be overexpressed in FOG-2^{R3K5A} hearts. Notably, the cell cycle inhibitor p21^{cip1} (encoded by *Cdkn1a*), a cell cycle inhibitor that binds to G1 and M CDK-cyclin complexes and inhibits their function to drive forward the cell cycle (Ahuja et al., 2007), appeared to be over-expressed in FOG-2^{R3K5A} hearts, thus providing a potential gene target for FOG-2/NuRD that might explain the proliferation defect seen in FOG-2^{R3K5A} cardiomyocytes. To confirm these results, we used quantitative RTPCR to evaluate the expression of a panel of cell-cycle genes in FOG-2^{R3K5A} cardiomyocytes at E16.5 (Figure 6A). Consistent with our microarray results, we found that *Cdkn1a* is transcriptionally up-regulated 2.01 ± 0.24-fold in FOG-2^{R3K5A} hearts, while the expression of other cell-cycle regulators were unchanged, including other cell-cycle regulators suggested by our microarray analysis (*Mycn*, *Fgf9*, and *Fgfr2)*. The expression of *Cdkn1a* is known to be up-regulated by the p53 tumor suppressor gene (*Trp53*) in response to DNA damage, but *Cdkn1a* can also be regulated independently and is induced without need for the presence of p53 in other contexts, such as differentiation of murine erythroleukemia cells (Macleod et al., 1995). Notably, in FOG-2^{R3K5A} hearts, *Trp53* expression is unchanged (Figure 6A), and thus up-regulation of *Cdkn1a* in FOG-2^{R3K5A} hearts is p53-independent in this context.

The NuRD complex subunit MTA1 has been previously described at the *Cdkn1a* promoter independent of p53 in DNA damage response (Li et al., 2010), which supports the idea that *Cdkn1a* could be a target of NuRD during heart development as well. To determine if the *Cdkn1a* promoter may be a direct target of FOG-2/NuRD, we first analyzed the *Cdkn1a* promoter for potential DNA binding sites for the FOG-2 interacting protein GATA4. Analysis of the *Cdkn1a* promoter using the online software algorithm TESS (Transcription Element Search System) (Schung and Overton, 1998) revealed 28 putative GATA binding

sites in a 2kb fragment of the *Cdkn1a* promoter (data not shown). This result suggested that *Cdkn1a* was a potential direct target of GATA4 and thus may also be a target of FOG-2/NuRD in developing cardiomyocytes.

To demonstrate a direct effect of FOG-2 on the *Cdkn1a* promoter, we cloned the *Cdkn1a* promoter into the luciferase reporter vector pGL2basic and performed *in vitro* transient transfection assays in NIH3T3 mouse fibroblasts. As shown in Figure 6B, GATA4 is able to directly activate this promoter, and FOG-2 effectively represses GATA4-mediated transcriptional activation. FOG-2^{R3K5A}, however, fails to repress transcription from the *Cdkn1a* promoter, showing that its recruitment of the NuRD complex (which is expressed endogenously in these fibroblasts) is important for repression of the *Cdkn1a* promoter in this system (Figure 6B). Taken together, these results are consistent with a model in which the lack of FOG-2-mediated recruitment of the NuRD complex at the *Cdkn1a* promoter in FOG-2^{R3K5A} cardiomyocytes leads to abnormal activation of the *Cdkn1a* promoter, resulting in overexpression of $p21^{cip1}$ and the suppression of cardiomyocyte proliferation and a thin myocardial wall phenotype.

Rescue of myocardial compact zone development and function in FOG-2^{R3K5A} mice with genetic removal of Cdkn1a

To provide further evidence for the importance of the repression of *Cdkn1a* during heart development, we sought to rescue the FOG-2^{R3K5A} phenotype by genetically ablating the expression of $p21^{cip1}$. Mice that are deficient for *Cdkn1a* are viable and fertile, although they are radiation-sensitive (Komarova et al., 2000). No defects have been described in the developing myocardium of *Cdkn1a* deficient mice and histology of *Cdkn1a* deficient hearts at birth is indistinguishable from that of wild type siblings (compare panels A & B in Figure 7). Thus, loss of this cell cycle inhibitor alone does not cause over-proliferation and thickening of the ventricular wall. We next crossed FOG-2^{R3K5A} mice to *Cdkn1a* null mice in order to obtain FOG-2^{R3K5A}; *Cdkn1a*$^{-/-}$ double mutant mice. As we showed previously, FOG-2^{R3K5A} hearts have a thin compact zone (Figure 7C), while FOG-2^{R3K5A}; *Cdkn1a*$^{-/-}$ double mutants have a significantly thicker myocardial compact zone at birth (compare panels C & D in Figure 7). However, wall thickness in the double mutant mice is still not completely normal, with only a modest 26.8 ± 3.2% rescue of wall thickness ($p<0.0001$) when compared to the left ventricular wall of wild-type mice (Figure 7E).

To determine if this increase in wall thickness in the FOG-2^{R3K5A}; *Cdkn1a*$^{-/-}$ mice was functionally significant, we examined neonatal mice from double heterozygous crosses at P0 by echocardiography (Figure 8). As expected, wild-type and *Cdkn1a*$^{-/-}$ left ventricular function are not significantly different as determined by chamber dimensions or fractional shortening (Figure 8). Consistent with our results shown in Figure 2, FOG-2^{R3K5A} hearts have a reduction in systolic function as determined by fractional shortening. However, in FOG-2^{R3K5A}; *Cdkn1a*$^{-/-}$ hearts, left ventricular fractional shortening is preserved (Figure 8G), demonstrating that the increased wall thickness seen by histology in these mice does improve left ventricular function. However, by postnatal day 14, the survival of FOG-2^{R3K5A}; *Cdkn1a*$^{-/-}$ is no better than that of their FOG-2^{R3K5A} siblings. This may be due to atrial and ventricular septal defects that are still present in the FOG-2^{R3K5A};

Cdkn1a$^{-/-}$ mice (Supplemental Figure 4). In addition, although fractional shortening is unchanged in the FOG-2^{R3K5A};*Cdkn1a*$^{-/-}$ mice, the left ventricular end diastolic dimension is slightly increased when compared to wild type mice (1.37 vs. 1.19 mm, p=0.07, Figure 8E), suggesting that these hearts are beginning to dilate and fail. Taken together, these results demonstrate that the ablation of *Cdkn1a* can partially compensate for the loss of FOG-2-NuRD interaction during cardiac development.

DISCUSSION

Gene regulation by chromatin remodeling is increasingly being appreciated to be important in the development of the mammalian heart (Bruneau, 2010; Han et al., 2011). In this report, we provide evidence to support the notion that the NuRD chromatin remodeling complex is also important for heart development. Our results demonstrate that when the NuRD complex is unable to interact with FOG-2 (and is thus unable to be recruited to FOG-2 target gene promoters) mice develop cardiac defects, which include atrial and ventricular septal defects as well as a thin ventricular myocardium. These defects result in left ventricular dysfunction and lead to death shortly after birth. We demonstrate that the thin myocardium is partially due to overexpression of the cell cycle inhibitor p21^{cip1}, and that the genetic ablation of *Cdkn1a* partially rescues the wall thickness defect and improves left ventricular function. We also show *Cdkn1a* is a target of FOG-2/NuRD transcriptional repression in NIH3T3 fibroblasts, thus defining a chromatin remodeling dependent molecular pathway for the regulation of cell cycle control during cardiac development.

The morphologic defects seen in the FOG-2^{R3K5A} mice are only a subset of those seen in mice with a complete disruption of the gene encoding FOG-2. FOG-2 deficient mice die between E13.5 and E14.5 with defects in cardiac development that include hyperplastic endocardial cushions, an overriding aorta, a common AV valve, atrial and ventricular septal defects, hypoplastic ventricular walls, and a failure to form the coronary vascular plexus (Svensson et al., 2000b; Tevosian et al., 2000). In the FOG-2^{R3K5A} mice, the endocardial cushions and atrioventricular valves appear normal, suggesting that the role FOG-2 plays in development of the heart valves may not be dependent on its interaction with the NuRD complex. In addition, FOG-2/NuRD interactions also do not appear to be necessary for the development of coronary vascular plexus, as there is only a slight delay in their development in FOG-2^{R3K5A} mice (see Supplemental Figure 2). NuRD independent functions of FOG-2 may be partially explained by the ability of FOG-2 to interact with other repressive factors such as C-terminal binding protein (CtBP) or COUP-TFII (Holmes et al., 1999; Huggins et al., 2001; Svensson et al., 2000a), but it is unclear what role these interactions may play during cardiac development.

The NuRD complex is likely to also play other roles in the development of the heart other than those we have observed due to disruption of its interaction with FOG-2. FOG-1 is also expressed in the valves of the developing heart and its loss leads to cardiac defects reminiscent of those seen in the endocardial cushions of FOG-2 deficient mice (Katz et al., 2003; Svensson et al., 2000b; Tevosian et al., 2000). The co-expression of both FOG-1 and FOG-2 in the developing valves suggests that FOG-1 may also mediate some NuRD-dependent function in this tissue, and that FOG-1/NuRD may play redundant roles with

FOG-2/NuRD. Redundancy of FOG/NuRD function may also explain the lack of a phenotype in the developing valves of FOG-2^{R3K5A} mice. It is also likely that there are FOG-independent functions of NuRD via NuRD's interaction with other transcriptional regulators during heart development. The N-terminal repression motif of FOG proteins that mediates interaction with the NuRD complex is also found in several other transcriptional repressors that are known to be involved in heart development, notably SALL1 and SALL4, the causative genes of Okihiro syndrome and Townes-Brokes, respectively (Kiefer et al., 2008; Lin et al., 2004; Sakaki-Yumoto et al., 2006). It is possible that at least part of the role of SALLs in heart development is also mediated by its interaction with the NuRD complex.

The function of FOG-2/NuRD to repress *Cdkn1a* transcription in the developing myocardium fits into a broader picture describing the regulation of the cardiomyocyte cell cycle during cardiac development. It has previously been shown that GATA4 activates expression of cell cycle proliferation genes, specifically *Cdk4* and *Ccnd2* (Cyclin D2) in the developing heart (Rojas et al., 2008). Previous work has also shown that GATA4 and GATA5 negatively regulate *Cdkn2c* (p18), *Cdkn1a* (p21^{cip1}), *Cdkn1b* (p27), and *Cdkn1c* (p57) in cardiomyocytes, also leading to increased cell proliferation (Singh et al., 2010). Taken together, these results suggest GATA4 is a critical regulator of cardiomyocyte proliferation. We show that FOG-2/NuRD regulates the promoter of the cell cycle inhibitor *Cdkn1a* in the developing heart to mediate its transcriptional repression likely through FOG-2's interaction with GATA4. Interestingly, we do not see changes in levels of other cell cycle inhibitors in FOG-2^{R3K5A} hearts, suggesting that other mechanisms may be involved in the regulation of *Cdkn2c*, *Cdkn1b*, and *Cdkn1c* by GATA factors during cardiac development. The levels of p21^{cip1} are also known to increase in cardiomyocytes shortly after birth and are thought to be partially responsible for the withdrawal from the cell cycle of postnatal cardiomyocytes (Evans-Anderson et al., 2008; Poolman et al., 1998). The level of FOG-2 expression also changes postnatally; it is expressed at lower levels in the adult heart than in the embryonic heart (Kim et al., 2009). Thus, the postnatal increase in p21^{cip1} may be mediated by decreasing FOG-2 levels and lack of repression of *Cdkn1a* by FOG-2/NuRD.

Previously, transcriptional regulation of *Cdkn1a* has been shown to play a critical role in skeletal muscle development. During skeletal muscle regeneration, the transcription factor FoxK1 is important for proliferative ability and functions by repressing the expression of *Cdkn1a* (Hawke et al., 2003a; Hawke et al., 2003b). In FoxK1 deficient mice, skeletal muscle proliferation is impaired due to the overexpression of *Cdkn1a*. The amount that *Cdkn1a* is overexpressed in FoxK1-deficient skeletal muscle regeneration is similar to the level of overexpression of *Cdkn1a* that we observe in developing cardiomyocytes in FOG2^{R3K5A} hearts. Also, in FoxK1 deficient mice, skeletal muscle proliferation can be rescued by genetically ablating *Cdkn1a*. Unlike the complete proliferative rescue observed in these mice, the rescue that we observe in ventricular wall thickness when crossing FOG-2^{R3K5A} mice to *Cdkn1a* deficient mice is only partial. The lack of complete rescue suggests a more complex mechanism for cardiomyocyte cell cycle control by FOG-2/NuRD that is only partially dependent on the transcriptional repression of *Cdkn1a*.

In summary, we have defined a novel pathway involving the NuRD chromatin remodeling complex in cardiomyocyte cell cycle control through its interaction with FOG-2. This is likely just one of many roles that the NuRD complex is playing during cardiac development, but the further elucidation of these roles must await the generation and characterization of mice with cardiomyocyte specific deletions of the NuRD complex.

Supplementary Material

Refer to Web version on PubMed Central for supplementary material.

Acknowledgments

This work was supported by NIH grant R01-HL071063 (to E.C.S.). A. S. G. and M.B. were supported from NIH training grants T32-HD055164 and T32-HL007381.

REFERENCES

Ahuja P, Sdek P, MacLellan WR. Cardiac myocyte cell cycle control in development, disease, and regeneration. Physiol Rev. 2007; 87:521–544. [PubMed: 17429040]

Bruneau BG. The developmental genetics of congenital heart disease. Nature. 2008; 451:943–948. [PubMed: 18288184]

Bruneau BG. Chromatin remodeling in heart development. Curr Opin Genet Dev. 2010; 20:505–511. [PubMed: 20702085]

Crispino JD, Lodish MB, Thurberg BL, Litovsky SH, Collins T, Molkentin JD, Orkin SH. Proper coronary vascular development and heart morphogenesis depend on interaction of GATA-4 with FOG cofactors. Genes Dev. 2001; 15:839–844. [PubMed: 11297508]

Evans-Anderson HJ, Alfieri CM, Yutzey KE. Regulation of cardiomyocyte proliferation and myocardial growth during development by FOXO transcription factors. Circ Res. 2008; 102:686–694. [PubMed: 18218983]

Flagg AE, Earley JU, Svensson EC. FOG-2 attenuates endothelial-to-mesenchymal transformation in the endocardial cushions of the developing heart. Dev Biol. 2007; 304:308–316. [PubMed: 17274974]

Gao Z, Huang Z, Olivey HE, Gurbuxani S, Crispino JD, Svensson EC. FOG-1-mediated recruitment of NuRD is required for cell lineage re-enforcement during haematopoiesis. EMBO J. 2010a; 29:457–468. [PubMed: 20010697]

Gao Z, Kim GH, Mackinnon AC, Flagg AE, Bassett B, Earley JU, Svensson EC. Ets1 is required for proper migration and differentiation of the cardiac neural crest. Development. 2010b; 137:1543–1551. [PubMed: 20356956]

Han P, Hang CT, Yang J, Chang CP. Chromatin remodeling in cardiovascular development and physiology. Circ Res. 2011; 108:378–396. [PubMed: 21293009]

Hawke TJ, Jiang N, Garry DJ. Absence of p21CIP rescues myogenic progenitor cell proliferative and regenerative capacity in Foxk1 null mice. J Biol Chem. 2003a; 278:4015–4020. [PubMed: 12446708]

Hawke TJ, Meeson AP, Jiang N, Graham S, Hutcheson K, DiMaio JM, Garry DJ. p21 is essential for normal myogenic progenitor cell function in regenerating skeletal muscle. Am J Physiol Cell Physiol. 2003b; 285:C1019–1027. [PubMed: 12826599]

Holmes M, Turner J, Fox A, Chisholm O, Crossley M, Chong B. hFOG-2, a novel zinc finger protein, binds the co-repressor mCtBP2 and modulates GATA-mediated activation. J Biol Chem. 1999; 274:23491–23498. [PubMed: 10438528]

Hong W, Nakazawa M, Chen YY, Kori R, Vakoc CR, Rakowski C, Blobel GA. FOG-1 recruits the NuRD repressor complex to mediate transcriptional repression by GATA-1. EMBO J. 2005; 24:2367–2378. [PubMed: 15920470]

Huggins GS, Bacani CJ, Boltax J, Aikawa R, Leiden JM. Friend of GATA 2 physically interacts with chicken ovalbumin upstream promoter-TF2 (COUP-TF2) and COUP TF3 and represses COUP-TF2-dependent activation of the atrial natriuretic factor promoter. J Biol Chem. 2001; 276:28029–28036. [PubMed: 11382775]

Katz SG, Cantor AB, Orkin SH. Interaction between FOG-1 and the corepressor C-terminal binding protein is dispensable for normal erythropoiesis in vivo. Mol Cell Biol. 2002; 22:3121–3128. [PubMed: 11940669]

Katz SG, Williams A, Yang J, Fujiwara Y, Tsang AP, Epstein JA, Orkin SH. Endothelial lineage-mediated loss of the GATA cofactor Friend of GATA 1 impairs cardiac development. Proc Natl Acad Sci U S A. 2003; 100:14030–14035. [PubMed: 14614148]

Kiefer SM, Robbins L, Barina A, Zhang Z, Rauchman M. SALL1 truncated protein expression in Townes-Brocks syndrome leads to ectopic expression of downstream genes. Hum Mutat. 2008; 29:1133–1140. [PubMed: 18470945]

Kim GH, Samant SA, Earley JU, Svensson EC. Translational control of FOG-2 expression in cardiomyocytes by microRNA-130a. PLoS One. 2009; 4:e6161. [PubMed: 19582148]

Knowlton KU, Baracchini E, Ross RS, Harris AN, Henderson SA, Evans SM, Glembotski CC, Chien KR. Co-regulation of the atrial natriuretic factor and cardiac myosin light chain-2 genes during alpha-adrenergic stimulation of neonatal rat ventricular cells. Identification of cis sequences within an embryonic and a constitutive contractile protein gene which mediate inducible expression. J Biol Chem. 1991; 266:7759–7768. [PubMed: 1850419]

Komarova EA, Christov K, Faerman AI, Gudkov AV. Different impact of p53 and p21 on the radiation response of mouse tissues. Oncogene. 2000; 19:3791–3798. [PubMed: 10949934]

Lejon S, Thong SY, Murthy A, AlQarni S, Murzina NV, Blobel GA, Laue ED, Mackay JP. Insights into association of the NuRD complex with FOG-1 from the crystal structure of an RbAp48.FOG-1 complex. J Biol Chem. 2011; 286:1196–1203. [PubMed: 21047798]

Li C, Wong WH. Model-based analysis of oligonucleotide arrays: expression index computation and outlier detection. Proc Natl Acad Sci U S A. 2001; 98:31–36. [PubMed: 11134512]

Li DQ, Pakala SB, Reddy SD, Ohshiro K, Peng SH, Lian Y, Fu SW, Kumar R. Revelation of p53-independent function of MTA1 in DNA damage response via modulation of the p21 WAF1-proliferating cell nuclear antigen pathway. J Biol Chem. 2010; 285:10044–10052. [PubMed: 20071335]

Lin AC, Roche AE, Wilk J, Svensson EC. The N termini of Friend of GATA (FOG) proteins define a novel transcriptional repression motif and a superfamily of transcriptional repressors. J Biol Chem. 2004; 279:55017–55023. [PubMed: 15507435]

Liu P, Jenkins NA, Copeland NG. A highly efficient recombineering-based method for generating conditional knockout mutations. Genome Res. 2003; 13:476–484. [PubMed: 12618378]

Lu JR, McKinsey TA, Xu H, Wang DZ, Richardson JA, Olson EN. FOG-2, a heart- and brain-enriched cofactor for GATA transcription factors. Mol Cell Biol. 1999; 19:4495–4502. [PubMed: 10330188]

Macleod KF, Sherry N, Hannon G, Beach D, Tokino T, Kinzler K, Vogelstein B, Jacks T. p53-dependent and independent expression of p21 during cell growth, differentiation, and DNA damage. Genes Dev. 1995; 9:935–944. [PubMed: 7774811]

Miccio A, Wang Y, Hong W, Gregory GD, Wang H, Yu X, Choi JK, Shelat S, Tong W, Poncz M, Blobel GA. NuRD mediates activating and repressive functions of GATA-1 and FOG-1 during blood development. EMBO J. 2010; 29:442–456. [PubMed: 19927129]

Poolman RA, Gilchrist R, Brooks G. Cell cycle profiles and expressions of p21CIP1 AND P27KIP1 during myocyte development. Int J Cardiol. 1998; 67:133–142. [PubMed: 9891946]

Roche AE, Bassett BJ, Samant SA, Hong W, Blobel GA, Svensson EC. The zinc finger and C-terminal domains of MTA proteins are required for FOG-2-mediated transcriptional repression via the NuRD complex. J Mol Cell Cardiol. 2008; 44:352–360. [PubMed: 18067919]

Rojas A, Kong SW, Agarwal P, Gilliss B, Pu WT, Black BL. GATA4 is a direct transcriptional activator of cyclin D2 and Cdk4 and is required for cardiomyocyte proliferation in anterior heart field-derived myocardium. Mol Cell Biol. 2008; 28:5420–5431. [PubMed: 18591257]

Sakaki-Yumoto M, Kobayashi C, Sato A, Fujimura S, Matsumoto Y, Takasato M, Kodama T, Aburatani H, Asashima M, Yoshida N, Nishinakamura R. The murine homolog of SALL4, a causative gene in Okihiro syndrome, is essential for embryonic stem cell proliferation, and cooperates with Sall1 in anorectal, heart, brain and kidney development. Development. 2006; 133:3005–3013. [PubMed: 16790473]

Schung, J.; Overton, GC. TESS: Transcription Element Search Software on the WWW. 1998.

Singh MK, Li Y, Li S, Cobb RM, Zhou D, Lu MM, Epstein JA, Morrisey EE, Gruber PJ. Gata4 and Gata5 cooperatively regulate cardiac myocyte proliferation in mice. J Biol Chem. 2010; 285:1765–1772. [PubMed: 19889636]

Svensson EC, Huggins GS, Dardik FB, Polk CE, Leiden JM. A functionally conserved N-terminal domain of the friend of GATA-2 (FOG-2) protein represses GATA4-dependent transcription. J Biol Chem. 2000a; 275:20762–20769. [PubMed: 10801815]

Svensson EC, Huggins GS, Lin H, Clendenin C, Jiang F, Tufts R, Dardik FB, Leiden JM. A syndrome of tricuspid atresia in mice with a targeted mutation of the gene encoding Fog-2. Nat Genet. 2000b; 25:353–356. [PubMed: 10888889]

Svensson EC, Tufts RL, Polk CE, Leiden JM. Molecular cloning of FOG-2: a modulator of transcription factor GATA-4 in cardiomyocytes. Proc Natl Acad Sci U S A. 1999; 96:956–961. [PubMed: 9927675]

Tevosian SG, Deconinck AE, Cantor AB, Rieff HI, Fujiwara Y, Corfas G, Orkin SH. FOG-2: A novel GATA-family cofactor related to multitype zinc-finger proteins Friend of GATA-1 and U-shaped. Proc Natl Acad Sci U S A. 1999; 96:950–955. [PubMed: 9927674]

Tevosian SG, Deconinck AE, Tanaka M, Schinke M, Litovsky SH, Izumo S, Fujiwara Y, Orkin SH. FOG-2, a cofactor for GATA transcription factors, is essential for heart morphogenesis and development of coronary vessels from epicardium. Cell. 2000; 101:729–739. [PubMed: 10892744]

Tichopad A, Dilger M, Schwarz G, Pfaffl MW. Standardized determination of real-time PCR efficiency from a single reaction set-up. Nucleic Acids Res. 2003; 31:e122. [PubMed: 14530455]

Wade PA, Jones PL, Vermaak D, Wolffe AP. A multiple subunit Mi-2 histone deacetylase from Xenopus laevis cofractionates with an associated Snf2 superfamily ATPase. Curr Biol. 1998; 8:843–846. [PubMed: 9663395]

Xue Y, Wong J, Moreno GT, Young MK, Cote J, Wang W. NURD, a novel complex with both ATP-dependent chromatin-remodeling and histone deacetylase activities. Mol Cell. 1998; 2:851–861. [PubMed: 9885572]

Zhang Y, LeRoy G, Seelig HP, Lane WS, Reinberg D. The dermatomyositis-specific autoantigen Mi2 is a component of a complex containing histone deacetylase and nucleosome remodeling activities. Cell. 1998; 95:279–289. [PubMed: 9790534]

Highlights

1. A specific mutation in FOG-2 (FOG-2^{R3K5A}) disrupts FOG-2/NuRD interaction.
2. FOG-2 ^{R3K5A} mice die shortly after birth due to heart failure.
3. FOG-2/NuRD interaction is required for cardiomyocyte proliferation.
4. *Cdkn1a* is a target of FOG-2/NuRD and is overexpressed in FOG-2 ^{R3K5A} hearts.
5. Gene deletion of *Cdkn1a* partially rescues the phenotype of FOG-2^{R3K5A} mice.

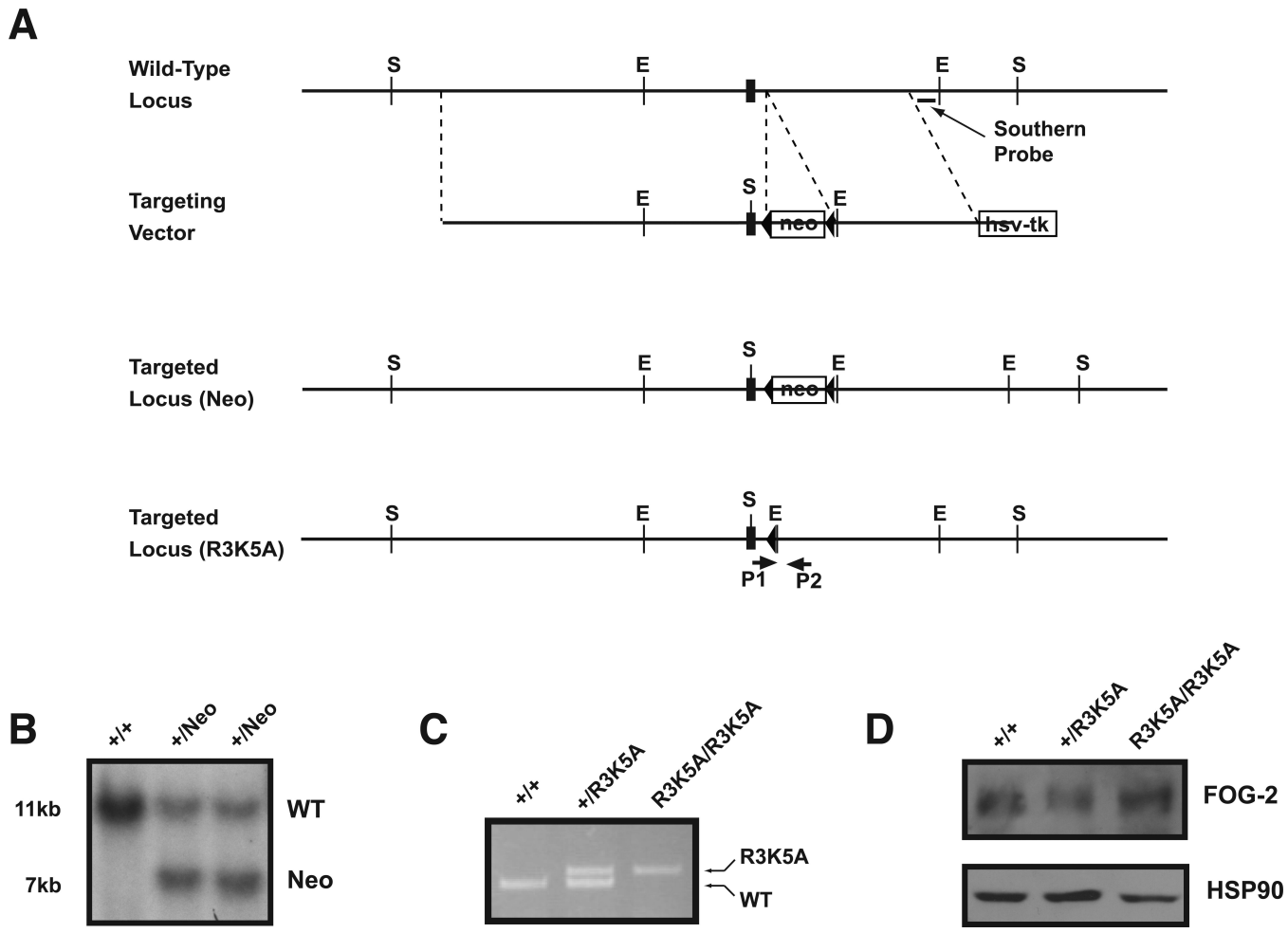

Figure 1. Generation of FOG-2^{R3K5A} mice

In (A), a schematic of the targeting strategy for generation of FOG-2^{R3K5A} animals centered on the first exon of the *Zfpm2* gene, represented by a black box. E = EcoRI restriction site, S = SacI restriction site, black triangles = position of LoxP sites, neo = neomycin resistance cassette. In (B), Southern analysis of tail DNA from offspring of chimeric mice, using the indicated probe and EcoRI restriction digestion, demonstrating germline transmission of the targeted locus. In (C), PCR assay from mouse genomic DNA using primers P1 and P2 showing expected size bands for wild-type (WT) and R3K5A allele. (D) Western blot of embryonic day 13.5 heart lysate using an antibody against FOG-2 (top panel) or heat shock protein 90 as a loading control (HSP90, bottom panel), demonstrating no qualitative change in the levels of FOG-2 in wild-type, heterozygous, or R3K5A homozygous mutant hearts.

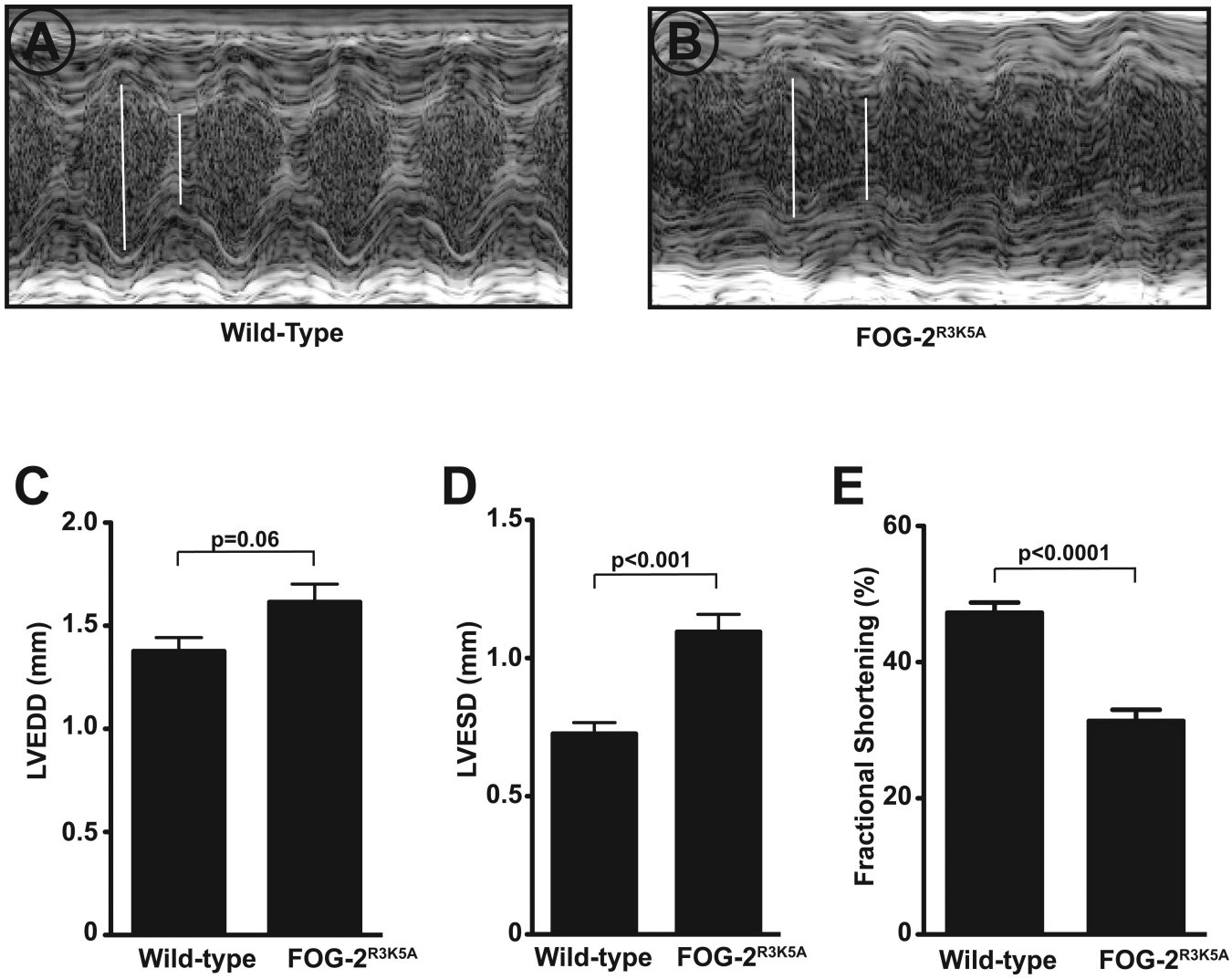

Figure 2. FOG-2^{R3K5A} mice have Left Ventricular Dysfunction at Birth

Echocardiographic M-mode tracings of (A) wild-type and (B) FOG-2^{R3K5A} newborn mice. Arrows indicate left ventricular end diastolic dimension (LVEDD) and left ventricular end systolic dimension (LVESD). In (C-E), quantification of LVEDD, LVESD, and fractional shortening of wild-type and FOG-2^{R3K5A} mice expressed as the mean ± S.E.M. (n=6), demonstrating a significant increase in LVESD and a significant reduction in fractional shortening of FOG-2^{R3K5A} mice.

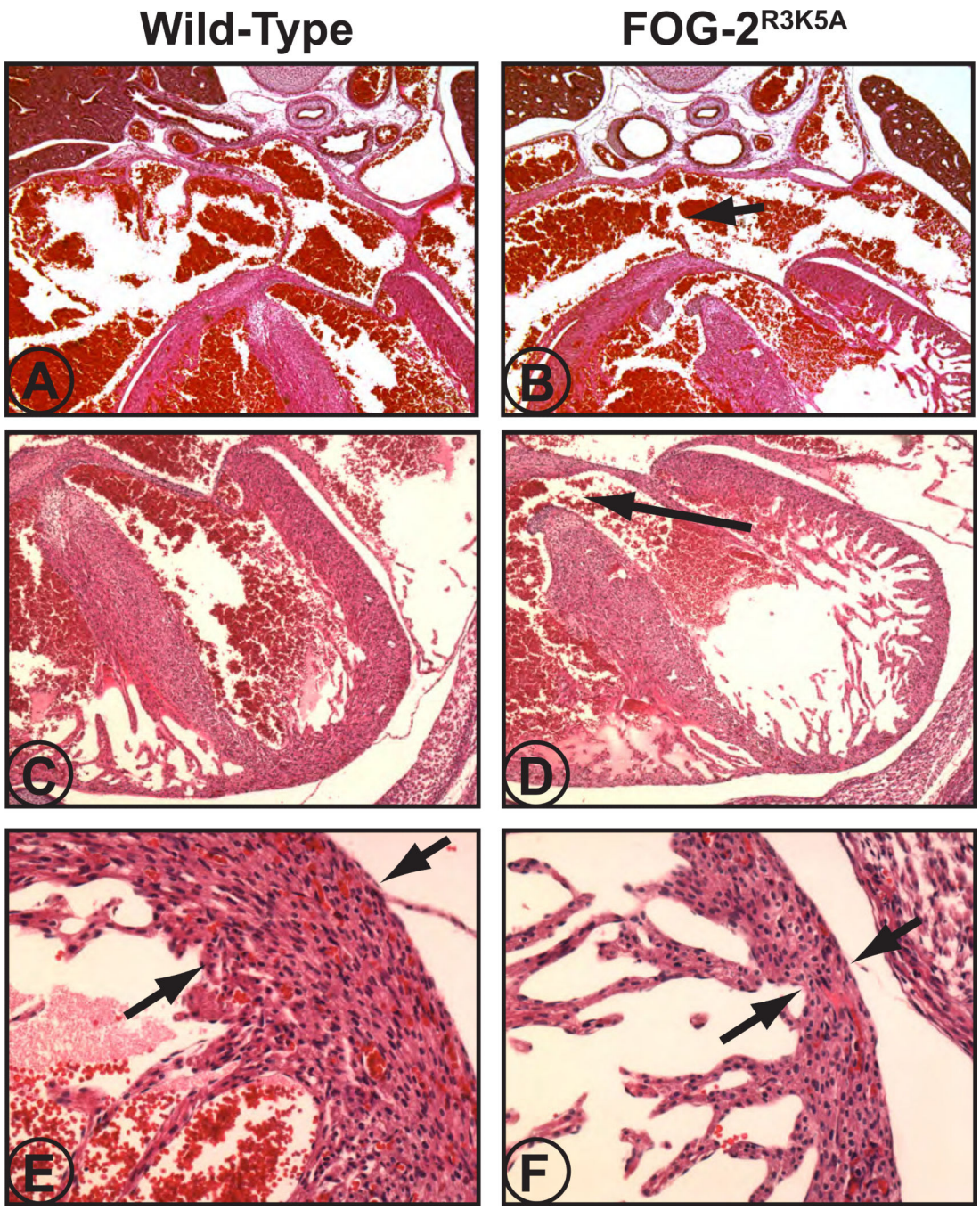

Figure 3. FOG-2^{R3K5A} mice have Atrial and Ventricular Septal Defects and a Dilated Cardiomyopathy at Birth

Wild-type (A, C, E) and FOG-2^{R3K5A} (B, D, F) mice were harvested at postnatal day 3 and transverse sections through the heart prepared and stained with hematoxylin and eosin. Note the atrial septal defect (B, arrow) and ventricular septal defect (D, arrow) in the FOG-2^{R3K5A} mice, and the thin LV myocardial wall (indicated by arrows in panels E and F). LV= Left Ventricle, RV=Right Ventricle.

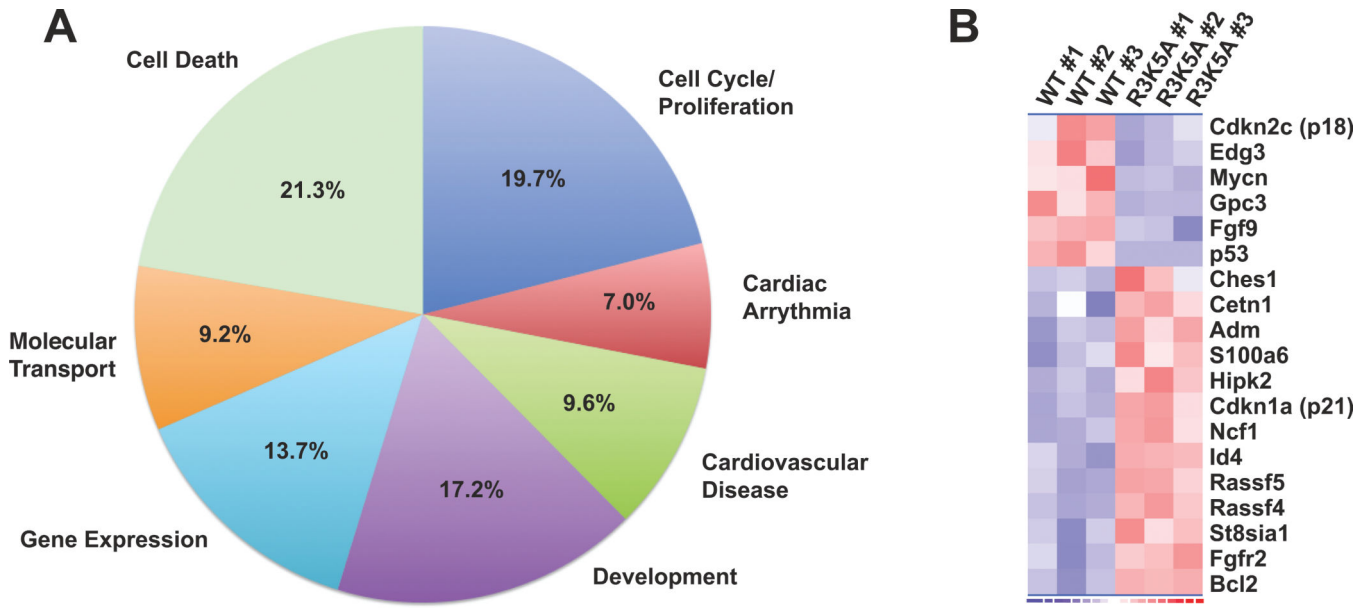

Figure 4. Microarray Analysis of FOG-2^{R3K5A} Hearts demonstrates Misregulation of Cell Cycle Related Genes

In (A), percentage of genes in the indicated super-networks as determined by Ingenuity Pathway Analysis. In (B), a heatmap for cell cycle and proliferation related genes that are misregulated more than 1.3-fold in hearts of FOG-2^{R3K5A} mice. Expression levels for each gene are standardized to a mean of 0 and standard deviation of 1; pure red represents a standardized expression level of 3 or more, and pure blue represents −3 or lower. The range of hues is visible in the scale at the bottom of the figure.

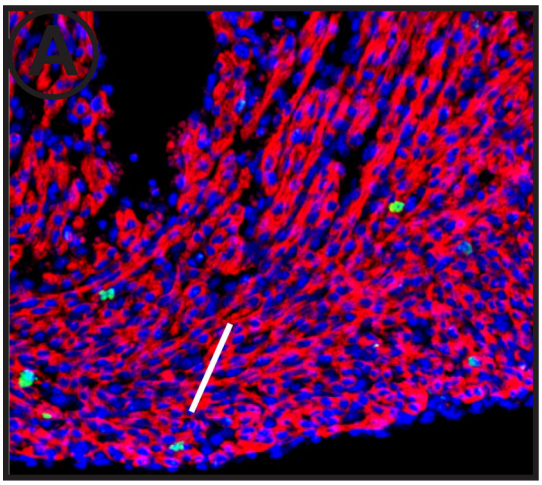

Wild-Type

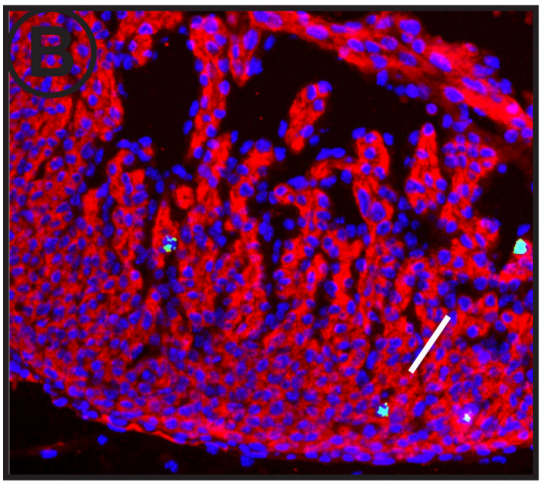

FOG-2^{R3K5A}

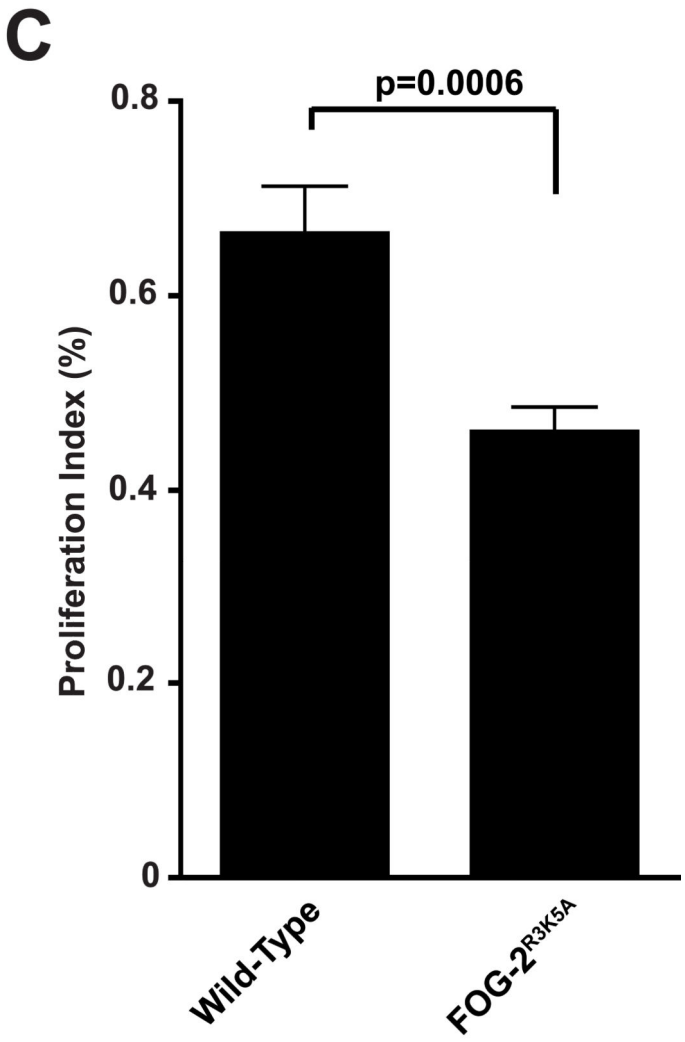

Figure 5. Proliferation in FOG-2^{R3K5A} Ventricular Myocardium is Decreased

Representative sections of embryonic day 16.5 wild-type (A) and FOG-2^{R3K5A} (B) hearts subject to immunofluorescence using an anti-phospho-histone H3 antibody to detect proliferating cells (green), and antibody to MF-20 to define myocytes (red), and counterstaining with DAPI to detect nuclei (blue). Arrows indicate phospho-histone H3 positive cells. In (C), quantification of the proportion of proliferating cardiomyocytes compared to the total number of cells in the ventricular myocardium (proliferation index) expressed as the mean ± S.E.M. At least seven depth-matched sections from three pairs of wild-type and three FOG-2^{R3K5A} hearts were analyzed.

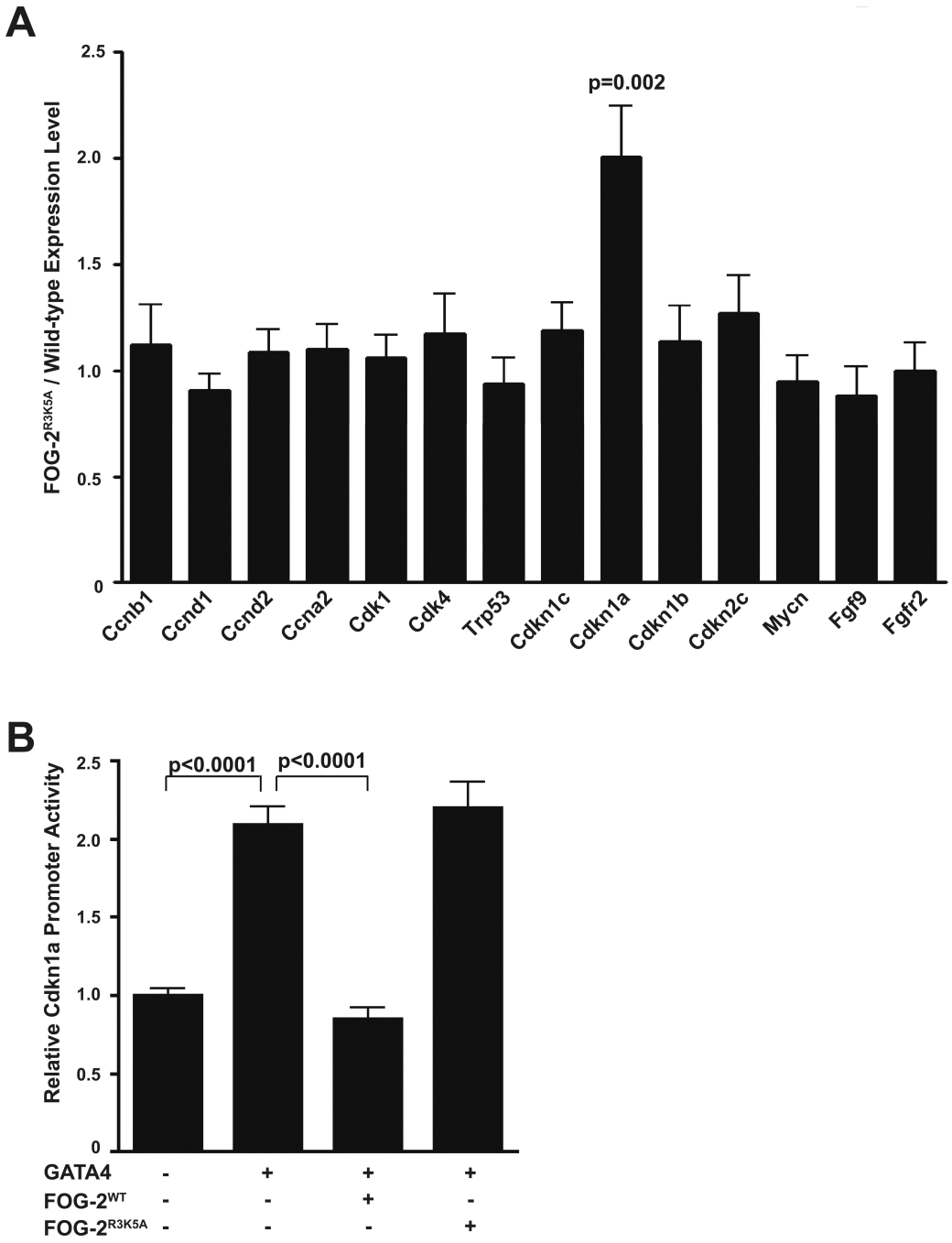

Figure 6. *Cdkn1a* is a Direct Target Gene of FOG-2/NuRD Chromatin Remodeling

In (A), total RNA was isolated from wild-type and FOG-2^{R3K5A} E16.5 hearts and subject to quantitative RT-PCR using primers specific for a panel of cell cycle genes. Results were normalized to expression of *Gapdh* and are expressed as the mean ± S.E.M. of the ratio of expression levels observed in FOG-2^{R3K5A} vs. wild-type hearts. '**' indicates statistical significance ($p<0.01$). In (B), NIH3T3 fibroblasts were transiently transfected with a reporter vector containing the *Cdkn1a* promoter driving expression of luciferase. In addition, expression vectors for GATA4, FOG-2, and FOG-2^{R3K5A} were also included as indicated.

Forty-eight hours after transfection, cells were harvested and assayed for luciferase activity. Results were normalized for transfection efficiency, and reported as the mean ± S.E.M. (n=12) relative to the activity of the *Cdkn1a* promoter alone.

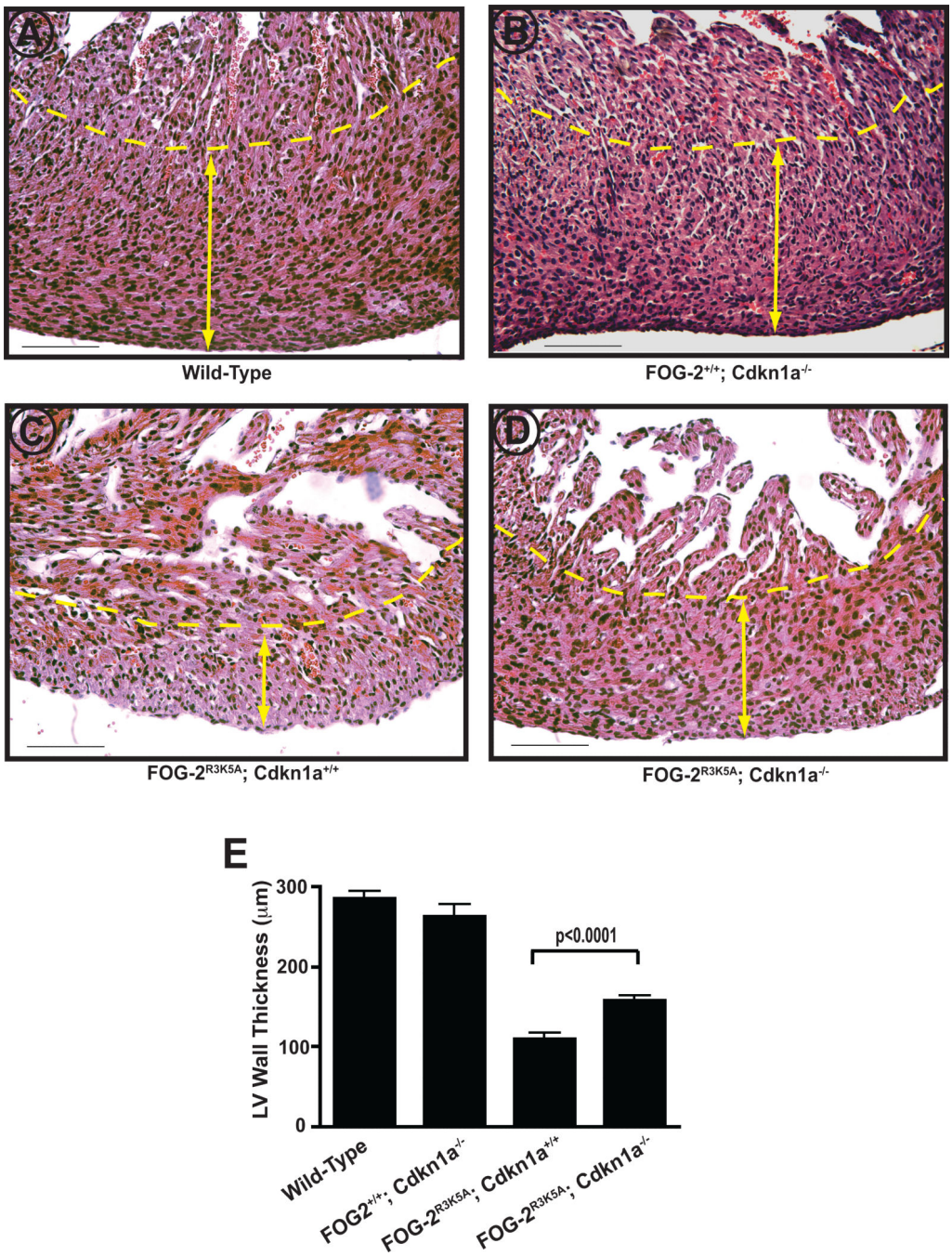

Figure 7. Inactivation of *Cdkn1a* Partially Rescues Ventricular Wall Thickness in FOG2^{R3K5A} Hearts

Mice deficient for *Cdkn1a* were crossed to FOG-2$^{R3K5A/+}$ mice to generate compound mutants. Pups from these crosses were harvested at birth and H&E stained histologic sections through the heart were prepared. Representative sections from wild-type, *Cdkn1a*$^{-/-}$, FOG-2^{R3K5A}; *Cdkn1a*$^{+/+}$, and FOG-2^{R3K5A}; *Cdkn1a*−/− mice are shown in panels (A-D), respectively. In each panel, the dashed line demarcates the boundary between the myocardial compact zone and the trabecular zone. Arrows demonstrate the thickness of the compact zone. In panel (E), quantification of left ventricular wall thickness of wild-type,

Cdkn1a$^{-/-}$, FOG-2^{R3K5A};*Cdkn1a*$^{+/+}$, and FOG-2^{R3K5A}; *Cdkn1a*$^{-/-}$ hearts expressed as the mean ± S.E.M. (n=24). Eight sections from 3 hearts of each genotype were analyzed.

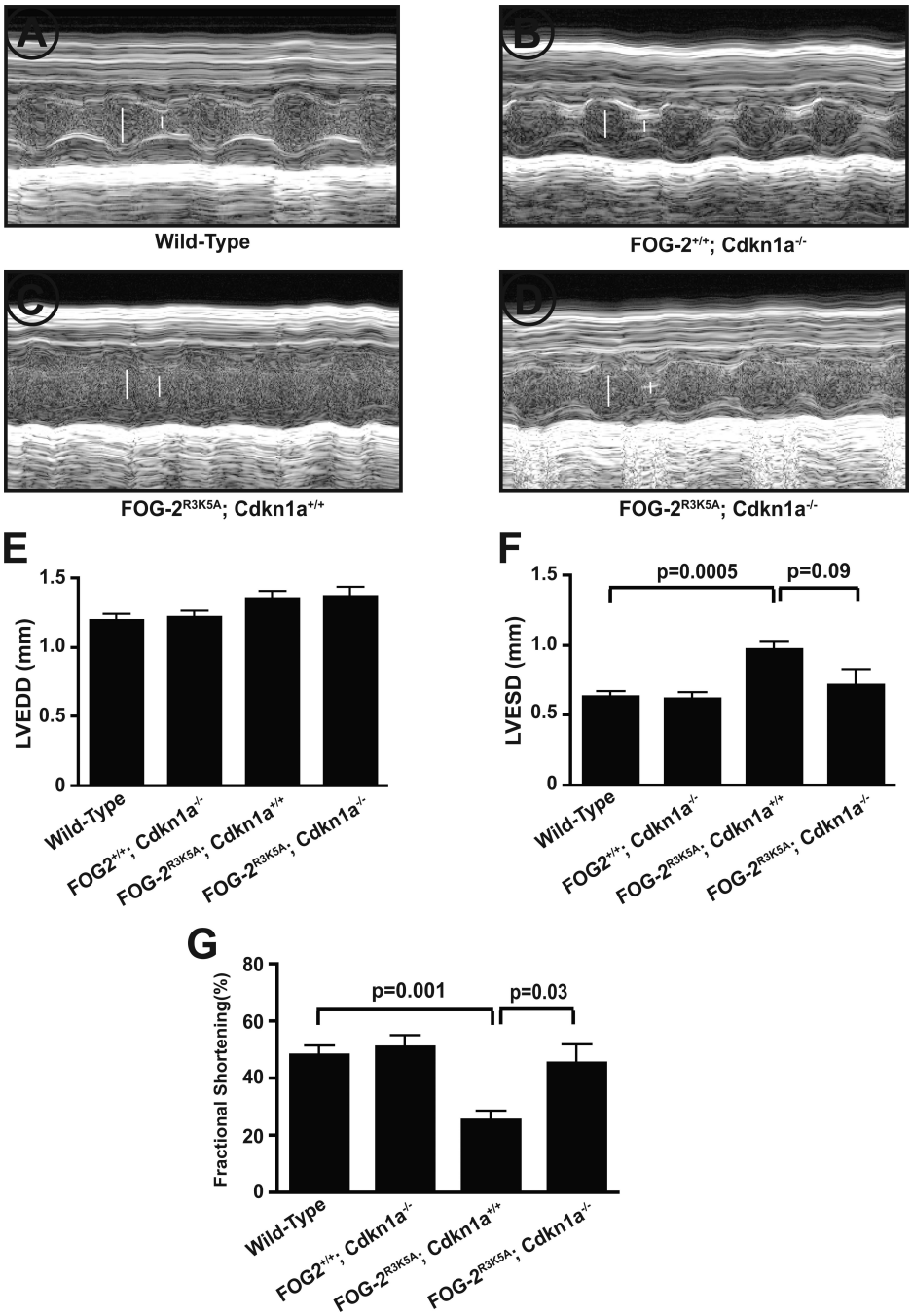

Figure 8. Inactivation of *Cdkn1a* Rescues Left Ventricular Function in FOG-2^{R3K5A} hearts

Representative M-mode echocardiography tracings from wild-type, *Cdkn1a*$^{-/-}$, FOG-2^{R3K5A};*Cdkn1a*$^{+/+}$, and FOG-2^{R3K5A}; *Cdkn1a*$^{-/-}$ mice at P0 are shown in panels (A-D), respectively. LVEDD (left ventricular end diastolic dimension) and LVESD (left ventricular end systolic dimension) are indicated by arrows. In (E-G), quantitation of the LVEDD, LVESD, and fractional shortening in all four genotypes. Values are expressed as

expressed as the mean ± S.E.M. Wild-type (n=10), *Cdkn1a*$^{-/-}$ (n=7), FOG-2^{R3K5A}; *Cdkn1a*$^{+/+}$ (n=4), FOG-2^{R3K5A}; *Cdkn1a*$^{-/-}$ (n=4).

Table 1

Genotype Analysis of Progeny from FOG-2$^{R3K5A/+}$ Heterozygous Crosses. FOG-2^{R3K5A} mice were crossed and resultant mice harvested as embryos (E13.5-E18.5), as newborns (P0-P3), or at weaning (P14-P21) and genotyped using a PCR-based assay.

Genotype	+/+	R3K5A/+	R3K5A/R3K5A
Embryonic	35 (29%)	54 (45%)	30 (25%)
Newborn	25 (33%)	39 (51%)	12 (16%)
Weaning	42 (33%)	82 (65%)	2 (2%)